Title
Tuning magnetic anisotropy of epitaxial Ag/Fe/Fe0.5Co0.5/MgO(001) films

Journal
Journal of Applied Physics, 124(15)

ISSN
0021-8979

Authors
Gao, N
Ge, C
Li, Q
et al.

Publication Date
2018-10-21

DOI
10.1063/1.5052297

Peer reviewed

Journal of Applied Physics

Tuning magnetic anisotropy of epitaxial Ag/Fe/$Fe_{0.5}Co_{0.5}$/MgO(001) films

Cite as: J. Appl. Phys. **124**, 153904 (2018); https://doi.org/10.1063/1.5052297
Submitted: 16 August 2018 . Accepted: 18 September 2018 . Published Online: 18 October 2018

N. Gao, C. Ge, Q. Li, M. Yang, C. Hwang, and Z. Q. Qiu

Tuning magnetic anisotropy of epitaxial Ag/Fe/$Fe_{0.5}Co_{0.5}$/MgO(001) films

N. Gao,[1] C. Ge,[1] Q. Li,[1] M. Yang,[1] C. Hwang,[2] and Z. Q. Qiu[1]
[1]*Department of Physics, University of California at Berkeley, Berkeley, California 94720, USA*
[2]*Korea Research Institute of Standards and Science, Yuseong, Daejeon 305-340, South Korea*

(Received 16 August 2018; accepted 18 September 2018; published online 18 October 2018)

Single crystalline Ag/Fe/$Fe_{0.5}Co_{0.5}$/MgO(001) films were grown by Molecular Beam Epitaxy and investigated by Magneto-Optic Kerr Effect (MOKE). We find that even though the 4-fold magnetic anisotropies of Ag/Fe/MgO(001) and Ag/$Fe_{0.5}Co_{0.5}$/MgO(001) films are different from the corresponding bulk values, their opposite signs allow a fine tuning of the 4-fold magnetic anisotropy in Ag/Fe/$Fe_{0.5}Co_{0.5}$/MgO(001) films by varying the Fe and $Fe_{0.5}Co_{0.5}$ film thicknesses. In particular, the critical point of zero anisotropy can be achieved in a wide range of film thicknesses. Using Rotational MOKE, we determined and constructed the anisotropy phase diagram in the Fe and $Fe_{0.5}Co_{0.5}$ thickness plane from which the zero anisotropy exhibits a linear relation between the Fe and $Fe_{0.5}Co_{0.5}$ thickness. *Published by AIP Publishing.* https://doi.org/10.1063/1.5052297

I. INTRODUCTION

Magnetic anisotropy plays an important role in spintronics because it determines many magnetic behaviors of magnetic nanostructures.[1] For example, the magnetic anisotropy in magnetic hard disks should define not only the stable magnetic direction for the binary memory bits but also an appropriate strength for thermal stability and magnetic writing process.[2,3] For magnetic thin films, there have been two categories in engineering magnetic anisotropy. One is to tune the spin axis perpendicular to the film plane, or the so-called spin reorientation transition (SRT) where the easy axis of spin changes from perpendicular to in-plane direction by varying temperature or film thickness.[4–6] The other is to tune the spin axis within the film plane by employing vicinal substrates,[7–10] magneto elastic coupling,[11] alloys, etc.

While perpendicular magnetic recording technology is widely utilized, in-plane spin engineering has potential applications in high density memories by employing multipole remanence states.[12,13] For example, a magnetic thin film with a cubic crystal structure consists of a 4-fold magnetic anisotropy which could stabilize the magnetization in four equivalent directions thus doubling the memory capacity as compared to binary states. It is therefore highly demanded to control and manipulate this 4-fold anisotropy in magnetic thin films, due to the competing requirements of state stability and low writing current. There are several approaches toward this goal. One is to find a system which has opposite signs of surface and bulk 4-fold anisotropies so that an in-plane SRT is expected at a critical film thickness.[14,15] Such SRT often happens at the sub-nanometer regime, limiting its application to a wide range of film thickness. The second approach employs ferromagnetic (FM)/antiferromagnetic (AFM) bilayers in which the interfacial coupling could switch the 4-fold easy axis of the FM layer.[16] However, FM/AFM interfacial coupling simultaneously induces a strong uniaxial anisotropy that could prohibit the 4-fold magnetization switching. In addition, the uncompensated spins at the AFM surface depend sensitively on the detailed surface roughness, making it difficult to have a fine tuning of the 4-fold anisotropy.[17,18] The other approach is to utilize magnetic alloys in which the two components have opposite magnetic anisotropies so that alloy composition could tune the magnetic anisotropy.[19,20] However, ultrathin films usually have a different anisotropy than the corresponding bulk materials so that it is hard to predesign the alloy composition before growing the thin film, making it difficult to apply this method to a wide range of film thicknesses.

In this paper, we use double layers of Ag/Fe/$Fe_{0.5}Co_{0.5}$/MgO(001) to tune the magnetic anisotropy. Fe, FeCo, and their bilayers combined with MgO are promising systems for magnetic tunnel junctions,[21,22] as well as for spin dynamics studies.[23–25] Previous works show that 4-fold magnetic anisotropies in body-centered cubic (bcc) Ag/Fe/MgO(001) and Ag/$Fe_{0.5}Co_{0.5}$/MgO(001) thin films have opposite signs but with their anisotropy values different from their bulk values.[22,26–28] By locking the magnetizations together as a single layer, we demonstrate that the in-plane 4-fold magnetic anisotropy in epitaxial Ag/Fe/$Fe_{0.5}Co_{0.5}$/MgO(001) films can be easily tuned by varying the film thickness in a wide range.

II. EXPERIMENT

A 10×10 mm square shaped MgO(001) single crystalline substrate was ultrasonically cleaned in acetone and alcohol before being loaded into an ultra-high vacuum (UHV) chamber of base pressure of 4×10^{-10} Torr. After annealing at 530 °C for 8 h, the MgO(001) substrate exhibits sharp Low Energy Electron Diffraction (LEED) spots, indicating a well-defined (001) surface [Fig. 1(b)]. Fe ($0 \sim 6$ nm) and $Fe_{0.5}Co_{0.5}$ ($0 \sim 3$ nm) films were grown into cross wedges [Fig. 1(a)] at room temperature by moving the substrate behind a knife-edge shutter during the film growth. The $Fe_{0.5}Co_{0.5}$ film was deposited by co-evaporating Fe and Co from two e-beam evaporators. Finally, a 3 nm Ag film was grown on top of the bilayer to protect the sample from contamination. The epitaxial growth of the body-centered cubic (bcc) structure of Fe and $Fe_{0.5}Co_{0.5}$ films was confirmed by LEED patterns with the [001] axis parallel to the

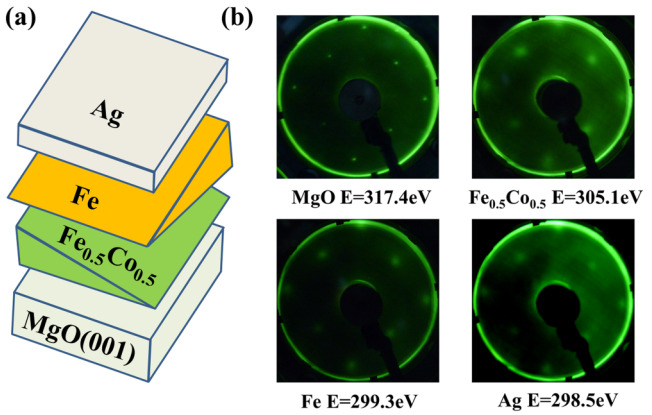

FIG 1. (a) Schematic drawing of a double wedged Ag/Fe/$Fe_{0.5}Co_{0.5}$/MgO(001). (b) LEED patterns of Ag(3 nm)/Fe(6 nm)/$Fe_{0.5}Co_{0.5}$(3 nm)/MgO(001).

MgO [110] axis [Fig. 1(b)]. The sample was taken out of the UHV chamber and measured by a table top Magneto-Optic Kerr Effect (MOKE) setup assembled with a vector magnet that can produce a magnetic field in any direction within the sample surface plane.[29]

III. RESULT AND DISCUSSION

We first show the hysteresis loops of a single layer of Fe (4.0 nm) and $Fe_{0.5}Co_{0.5}$ (2.5 nm), respectively, in the longitudinal MOKE mode with the laser incident plane parallel to the film [100] and [110] directions [Fig. 2(a)]. The Fe single layer hysteresis loop has a square shape with a full remanence for a light incident along [100], while the remanence drops and saturation field increases for a light incident along [110], showing that bcc Fe/MgO(001) film has its magnetization easy axis along [100] and [010] axes (i.e., a positive 4-fold magnetic anisotropy, $K_4 > 0$). The $Fe_{0.5}Co_{0.5}$ single layer hysteresis loop exhibits an opposite behavior, showing that bcc $Fe_{0.5}Co_{0.5}$/MgO(001) film has its magnetization easy axis along [110] and [$\bar{1}$10] axes (i.e., a negative 4-fold magnetic anisotropy, $K_4 < 0$).

We then show hysteresis loops of Fe/$Fe_{0.5}Co_{0.5}$/MgO(001) bilayers at 2.0 nm $Fe_{0.5}Co_{0.5}$ thickness (t_{FeCo} = 2.0 nm) and at different Fe thicknesses (t_{Fe}). The bilayer hysteresis loops have a single coercivity and a single saturation field, showing that the $Fe_{0.5}Co_{0.5}$ and Fe magnetizations are completely locked together by their interfacial magnetic coupling to behave as a single FM layer. For t_{Fe} = 2.0 nm, the bilayer hysteresis loop exhibits a hard-axis character [Fig. 2(b)], showing that the bilayer behavior is dominated by the $Fe_{0.5}Co_{0.5}$ film. For t_{Fe} = 6.0 nm, the bilayer hysteresis loop exhibits an easy-axis loop with a full remanence, showing that the bilayer behavior is dominated by the Fe film. The result of Fig. 2(b) implies that the bilayer magnetization easy axis should undergo a transition from the [110] axis to the [100] axis with increasing Fe film thickness. Since hysteresis loops do not give magnetic anisotropy directly, we performed Rotational MOKE (ROTMOKE) to determine the magnetic anisotropy quantitatively.

ROTMOKE is a MOKE version of magnetic torque measurement by rotating a magnetic field within the film

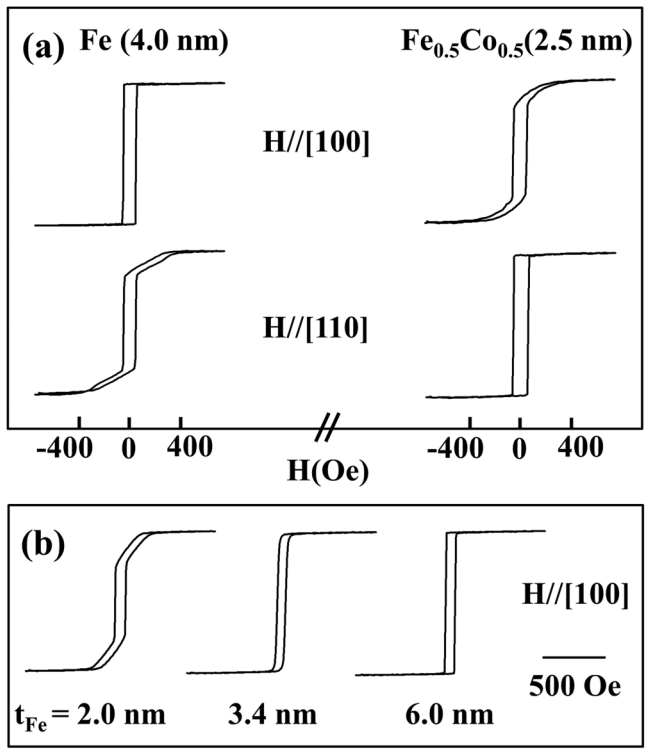

Fig 2. (a) Normalized hysteresis loops of Ag/Fe(4.0 nm)/MgO(001) and Ag/$Fe_{0.5}Co_{0.5}$(2.5 nm)/MgO(001) using longitudinal MOKE with light incident along [100] and [110] directions. The loop shape indicates that [100] is an easy axis for Fe and a hard axis for $Fe_{0.5}Co_{0.5}$. (b) Hysteresis loops of Ag/Fe(t_{Fe})/$Fe_{0.5}Co_{0.5}$(2.0 nm)/MgO(001) with a light incident along [100] direction. The loops change from hard axis to easy axis characteristics with increasing Fe thickness.

plane. Without any magnetic anisotropy, the rotating magnetic field should align the film magnetization exactly in the field direction. While in the presence of an in-plane magnetic anisotropy, the magnetization direction will deviate from the magnetic field direction as a result of lowering the magnetic anisotropy energy especially when the field is in the magnetic hard axis direction. Since MOKE measures the projection of the magnetization onto the optical plane, the magnetization direction can be obtained directly from ROTMOKE at a given magnetic field direction. Therefore, a determination of the angle between the magnetization and the magnetic field will in principle allow a determination of the magnetic anisotropy of the film. Such an extraction of anisotropy using ROTMOKE is more accurate than just comparing the coercivity from the hysteresis loops, since the latter might be affected by the intrinsic domain formation and the remanence of magnets used in the MOKE measurement.

To have a quantitative analysis, let us consider the free energy density *E* of a (001) thin film within a magnetic field H. Even though a perfect (001) thin film should contain only a 4-fold magnetic anisotropy (K_4), we include a uniaxial magnetic anisotropy (K_u) (e.g., step-induced uniaxial anisotropy) without losing generality. The free energy can be described by

$$E = -HM\cos(\theta - \varphi) + K_u \sin^2(\varphi - \varphi_0) + K_4 \sin^2\varphi \cos^2\varphi, \quad (1)$$

where M is the saturation magnetization of the film and φ, φ_0, and θ are the angles of the magnetization, uniaxial axis (easy axis for $K_u > 0$ and hard axis for $K_u < 0$), and applied field with respect to the light incidence plane [Fig. 3(a)], respectively. We also require that the applied field is strong enough to magnetize the film into a single domain state. Following the conventional definition, a positive (or negative) K_4 corresponds to a 4-fold easy (or hard) axis parallel to the [100] axis. By minimizing the free energy with respect to φ, it is easy to derive the magnetic torque $\left[|\vec{M} \times \vec{H}| = MH\sin(\theta - \varphi)\right]$ at equilibrium:

$$H\sin(\theta - \varphi) = \frac{1}{2}H_u \sin 2(\varphi - \varphi_0) + \frac{1}{4}H_4 \sin(4\varphi), \quad (2)$$

where $H_u = 2K_u/M$ and $H_4 = 2K_4/M$ are the uniaxial anisotropy field and the 4-fold anisotropy field, respectively. For each magnetic field angle θ, the magnetization angle φ and the magnetic torque $H\sin(\theta - \varphi)$ can be obtained from the normalized MOKE signal of cosφ. Then the relation between the magnetic torque $H\sin(\theta - \varphi)$ and the magnetization angle φ can be obtained from ROTMOKE measurement by rotating the magnetic field within the film plane. A fitting of the experimental data using Eq. (2) will retrieve the anisotropy fields of H_u and H_4. Figure 3(b) shows the data of the $H\sin(\theta - \varphi)$ vs φ and the fitting result for two samples of Ag/Fe(4.0 nm)/MgO(001) and Ag/$Fe_{0.5}Co_{0.5}$(2.5 nm)/MgO(001) single magnetic layers, respectively. The fitting results (red solid lines) yield $H_u = -54$ Oe, $\varphi_0 = 11°$, and $H_4 = 344$ Oe for Ag/Fe(4.0 nm)/MgO(001), and $H_u = -51$ Oe, $\varphi_0 = 7°$, and $H_4 = -252$ Oe for Ag/$Fe_{0.5}Co_{0.5}$(2.5 nm)/MgO(001). The small but non-zero uniaxial anisotropy is reflected by the deviation of the magnetic torque from a perfect 4-fold periodicity within the 360° range of φ. This small uniaxial anisotropy is very difficult to manifest in hysteresis loops but is conceivable by recognizing that single crystalline substrate usually contains a miscut angle within ±0.5° so that atomic steps on the vicinal surface could induce a small uniaxial magnetic anisotropy. Nevertheless, both systems are dominated by the much greater 4-fold anisotropy field so that we will neglect the uniaxial anisotropy in the following discussion. The positive and negative values of H_4 in Fe and $Fe_{0.5}Co_{0.5}$ films show that the magnetic easy axis in Fe and $Fe_{0.5}Co_{0.5}$ are along the 4-fold [100] and [110] axes, respectively, in agreement with the hysteresis loop result [Fig. 2(a)].

The 4-fold anisotropy of a single layer comes from the contributions from both the bulk and surface effects, as

$$K_{4,\,sl} = K_4^{(s)}/t + K_4^{(b)}, \quad (3)$$

where t is the film thickness, and $K_4^{(s)}$ and $K_4^{(b)}$ denote the surface and bulk contributions, respectively. By plotting $H_4Mt/2$ as a function of film thickness, one would expect a linear behavior with the slope being $K_4^{(b)}$ and the intersection at t = 0 being $K_4^{(s)}$.

Figures 3(c) and 3(d) indeed show such linear behavior from which we extract the anisotropy fields: $K_{4,Fe}^{(b)} = 4.26 \times 10^5\,\mathrm{erg/cm^3}$ and $K_{4,Fe}^{(s)} = -4.87 \times 10^{-2}\,\mathrm{erg/cm^2}$ for Fe, and $K_{4,FeCo}^{(b)} = -6.18 \times 10^5\,\mathrm{erg/cm^3}$ and $K_{4,FeCo}^{(s)} = 9.32 \times 10^{-2}\,\mathrm{erg/cm^2}$ for $Fe_{0.5}Co_{0.5}$, where we have adopted the saturation magnetization value of Fe to be $M_{Fe} = 1711\,\mathrm{emu/cm^3}$ and that of $Fe_{0.5}Co_{0.5}$ as $M_{FeCo} = 1910\,\mathrm{emu/cm^3}$.[30] It is interesting to note that $K_4^{(b)}$ of Fe is smaller than its bulk value, while $|K_4^{(b)}|$ of $Fe_{0.5}Co_{0.5}$ is larger than its bulk value. This is typical for epitaxial Fe and $Fe_{0.5}Co_{0.5}$ thin films on MgO, as reported in Refs. 22–26.

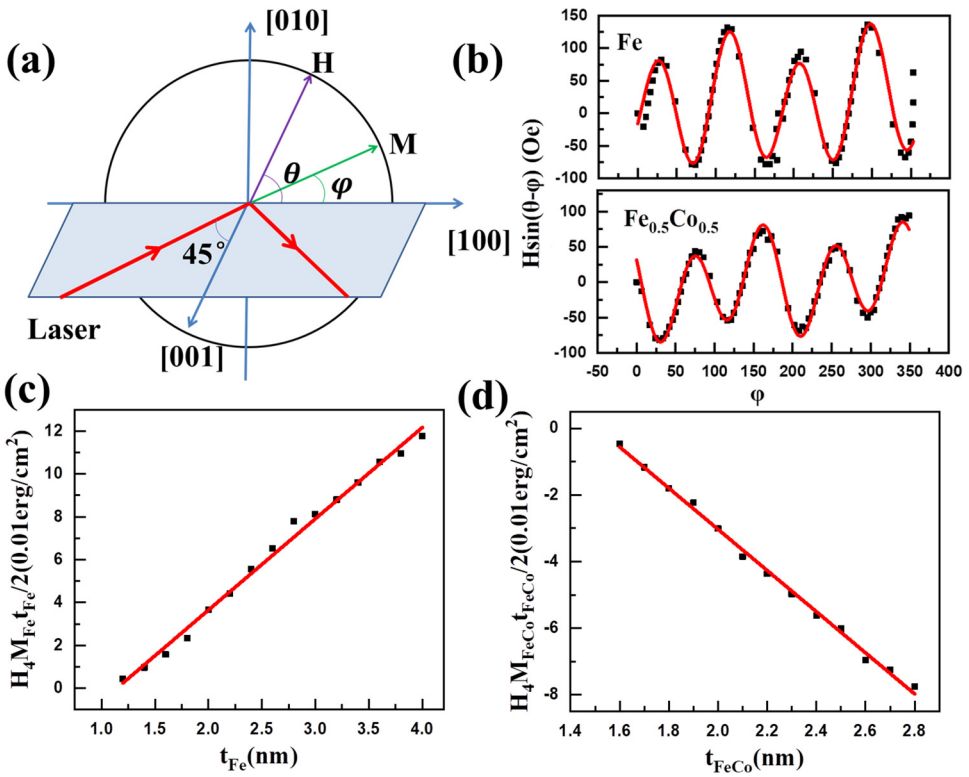

FIG 3. (a) Schematic illustration of the MOKE setup. Laser is incident in a plane perpendicular to the sample, and the incident angle is 45°. The incident plane intersects the sample plane in the Fe [100] direction. In the longitudinal MOKE mode, applied field sweeps along the [100] direction. In the ROTMOKE mode, applied field rotates a full 360° in the sample plane. (b) The RTOMOKE data of (top) Ag/Fe(4.0 nm)/MgO(001) and (bottom) Ag/$Fe_{0.5}Co_{0.5}$(2.5 nm)/MgO(001) are fitted (red solid lines) using Eq. (2) to extract the anisotropy field. (c) $H_4Mt/2$ of Ag/Fe/MgO(001) as a function of Fe thickness with linear fitting (red solid line). (d) $H_4Mt/2$ of Ag/$Fe_{0.5}Co_{0.5}$/MgO(001) as a function of $Fe_{0.5}Co_{0.5}$ thickness with linear fitting (red solid lines). The standard errors of fitted H4 and H2 in all the data points are within ±5 Oe.

The values of $K_4^{(s)}$ are on the same order as those obtained in Refs. 14 and 15. In addition, the opposite signs of $H_4^{(b)}$ and $H_4^{(s)}$ indicate the existence of an in-plane SRT of Fe and $Fe_{0.5}Co_{0.5}$ in the ultrathin regime as reported in Refs. 14 and 15.

We now present the ROTMOKE result of the bilayers. At fixed $Fe_{0.5}Co_{0.5}$ layer thickness of 2.5 nm, 2.0 nm, 1.5 nm, and 1.0 nm, Fig. 4(a) shows that increasing the Fe thickness changes the overall 4-fold anisotropy from negative to positive, confirming that the hysteresis loop change in Fig. 2(b) indeed corresponds to a transition of the 4-fold easy axis from [110] to [100] directions. The critical Fe thickness is larger for thicker $Fe_{0.5}Co_{0.5}$ bilayer films which is expected because more Fe is needed to balance the negative 4-fold anisotropy of thicker $Fe_{0.5}Co_{0.5}$. The H_4 for the films do not follow a linear dependence on Fe thickness.

Quantitatively, the 4-fold anisotropy field $H_{4,bl}$ for Fe/$Fe_{0.5}Co_{0.5}$ bilayer should be composed of both Fe and $Fe_{0.5}Co_{0.5}$ anisotropies weighted by their thicknesses and saturation magnetization:

$$H_{4,\,bl} = 2 \times \frac{K_{4,Fe}^{(b)} t_{Fe} + K_{4,FeCo}^{(b)} t_{FeCo} + K_{4,bl}^{(s)}}{t_{Fe} M_{Fe} + t_{FeCo} M_{FeCo}}, \qquad (4)$$

where $K_{4,Fe}^{(b)}$ ($K_{4,FeCo}^{(b)}$), t_{Fe} (t_{FeCo}), and M_{Fe} (M_{FeCo}) are the anisotropy constant, thickness, and saturation magnetization of Fe ($Fe_{0.5}Co_{0.5}$) layer, respectively, and $K_{4,bl}^{(s)}$ is the total interface contributions from $Fe_{0.5}Co_{0.5}$/MgO, Fe/$Fe_{0.5}Co_{0.5}$, and Ag/Fe interfaces. For each fixed $Fe_{0.5}Co_{0.5}$ thickness, we plot $H_{4,\,bl}(t_{Fe}M_{Fe} + t_{FeCo}M_{FeCo})/2$ as a function of t_{Fe} which indeed exhibits a linear dependence on t_{Fe} [Fig. 4(b)]. We then obtained $K_{4,Fe}^{(b)}$ from the linear slope, and $K_{4,FeCo}^{(b)} t_{FeCo} + K_{4,bl}^{(s)}$ from the intercepts. Since we have curves corresponding to different $Fe_{0.5}Co_{0.5}$ thicknesses, by plotting the intercepts as a function of t_{Fe} and performing linear fitting, we can simultaneously extract $K_{4,FeCo}^{(b)}$ and $K_{4,bl}^{(s)}$, as shown in Fig. 4(c). The almost same slopes of the four data sets in Fig. 4(b) also show that the $K_{4,Fe}^{(b)}$ does not vary with $Fe_{0.5}Co_{0.5}$ thickness. The final result is $K_{4,Fe}^{(b)} = 4.02 \times 10^5\ \mathrm{erg/cm^3}$, $K_{4,FeCo}^{(b)} = -6.37 \times 10^5\ \mathrm{erg/cm^3}$, and $K_{4,bl}^{(s)} = -1.20 \times 10^{-3}\ \mathrm{erg/cm^2}$. Compared to the fitting results from Figs. 3(c) and 3(d), the $K_4^{(b)}$ values of Fe and $Fe_{0.5}Co_{0.5}$ in the bilayer agree with the values of the single layer within 6%. It is interesting to note that the three interface contributions compensate somehow each other to produce a much smaller $K_{4,bl}^{(s)}$ than that of the single layers.

To search for the $H_{4,\,bl} = 0$ which defines the in-plane transition of the magnetic easy axis (e.g., the most soft point of the magnetic anisotropy), we merge all data together and construct a phase diagram of the 4-fold anisotropy field in the Fe and $Fe_{0.5}Co_{0.5}$ thickness plane [Fig. 4(d)]. The narrow white ribbon corresponds to the thickness region which gives rise to the disappearance of $H_{4,\,bl}$. As expected, the transition thickness of Fe depends linearly on the $Fe_{0.5}Co_{0.5}$ thickness. We also plot the straight line of $K_{4,Fe}^{(b)} t_{Fe} + K_{4,FeCo}^{(b)} t_{FeCo} + K_{4,bl}^{(s)} = 0$ according to the previous fitting results in the figure (dashed line), and it overlaps with the white ribbon. This result illustrates that the 4-fold anisotropy of Ag/Fe/$Fe_{0.5}Co_{0.5}$/MgO can be conveniently tuned across a wide thickness range.

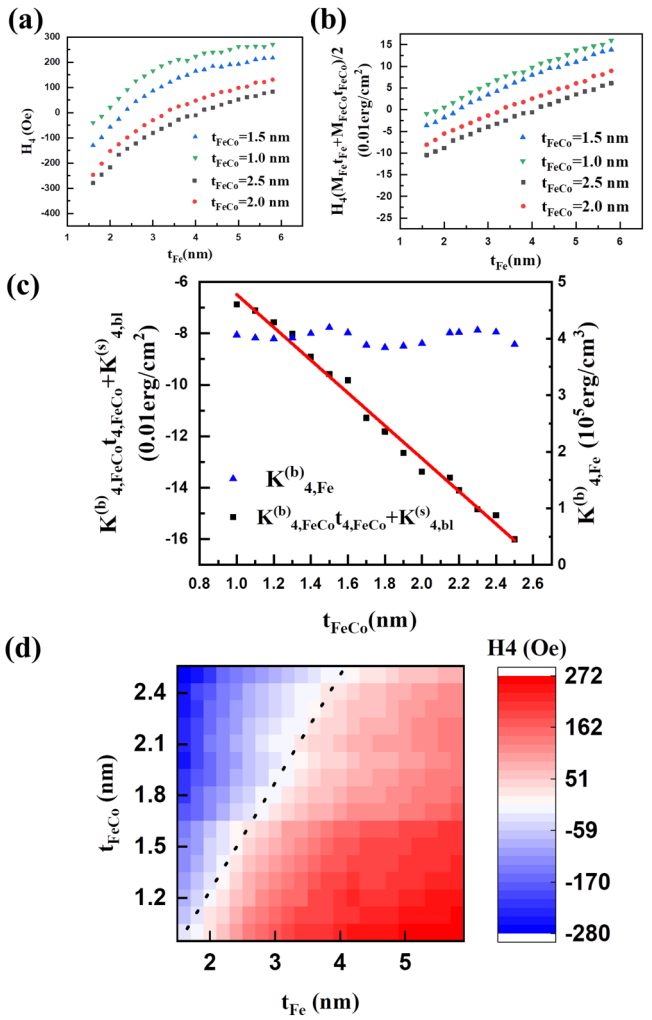

FIG 4. (a) The fitted H_4 of Ag/Fe/$Fe_{0.5}Co_{0.5}$/MgO(001) as a function of Fe thickness, with $Fe_{0.5}Co_{0.5}$ thickness being 2.5 nm, 2.0 nm, 1.5 nm, and 1.0 nm. (b) $H_{4,\,bl}(t_{Fe}M_{Fe} + t_{FeCo}M_{FeCo})/2$ as a function of t_{Fe} shows a linear dependence on the Fe thickness. (c) Linear fitting result of $K_{4,FeCo}^{(b)}$ using Eq. (4), as well as $K_{4,Fe}^{(b)}$ obtained in (b) for different t_{FeCo}. (d) Anisotropy field in the Fe and $Fe_{0.5}Co_{0.5}$ thickness plane. The white ribbon corresponds to the disappearance of H_4. The dashed line denotes the straight line of $K_{4,Fe}^{(b)} t_{Fe} + K_{4,FeCo}^{(b)} t_{FeCo} + K_{4,bl}^{(s)} = 0$.

IV. SUMMARY

In summary, we studied the 4-fold anisotropy of Ag/Fe/$Fe_{0.5}Co_{0.5}$/MgO(001) bilayers as a function of Fe and $Fe_{0.5}Co_{0.5}$ thicknesses using longitudinal MOKE and ROTMOKE. Contributions from bulk Fe, bulk $Fe_{0.5}Co_{0.5}$, and interfaces are extracted by fitting the thickness-dependent anisotropy field. We find that a 4-fold easy-axis transition of the in-plane magnetization occurs over a wide thickness range. Fine tuning of the 4-fold anisotropy via film thickness provides a simple and straightforward way to manipulate the easy magnetization axis within the film plane and might have potential applications in next generation spintronic devices.

ACKNOWLEDGMENTS

This work was supported by the US Department of Energy (DOE), Office of Science, Office of Basic Energy

Sciences, Materials Sciences and Engineering Division under Contract No. DE-AC02-05-CH11231 (van der Waals heterostructures program, KCWF16), the National Science Foundation (NSF) (Grant Nos. DMR-1504568 and DMR-1610060), the UC Office of the President Multicampus Research Programs and Initiatives (MRP-17-454963), the National Natural Science Foundation of China (NNSFC) (No. 61505243), the Future Materials Discovery Program through the National Research Foundation of Korea (No. 2015M3D1A1070467), and the Science Research Center Program through the National Research Foundation of Korea (No. 2015R1A5A1009962).

[1]S. A. Wolf, D. D. Awschalom, R. A. Buhrman, J. M. Daughton, S. von Molnár, M. L. Roukes, A. Y. Chtchelkanova, and D. M. Treger, Science **294**, 1488 (2001).
[2]S. N. Piramanayagam, J. Appl. Phys. **102**, 2 (2007).
[3]S. Ikeda, K. Miura, H. Yamamoto, K. Mizunuma, H. D. Gan, M. Endo, S. Kanai, J. Hayakawa, F. Matsukura, and H. Ohno, Nat. Mater. **9**, 721 (2010).
[4]D. P. Pappas, K. P. Kämper, and H. Hopster, Phys. Rev. Lett. **64**, 3179 (1990).
[5]Z. Q. Qiu, J. Pearson, and S. D. Bader, Phys. Rev. Lett. **70**, 1006 (1993).
[6]B. Schulz and K. Baberschke, Phys. Rev. B **50**, 13467 (1994).
[7]J. Chen and J. L. Erskine, Phys. Rev. Lett. **68**, 1212 (1992).
[8]W. Weber, C. H. Back, A. Bischof, D. Pescia, and R. Allenspach, Nature **374**, 788 (1995).
[9]Q. Li, T. Gu, J. Zhu, Z. Ding, J. X. Li, J. H. Liang, Y. M. Luo, Z. Hu, C. Y. Hua, H.-J. Lin, T. W. Pi, C. Won, and Y. Z. Wu, Phys. Rev. B **91**, 104424 (2015).
[10]J. X. Deng, A. Tan, J. Li, C. Hwang, and Z. Q. Qiu, J. Magn. Magn. Mater. **408**, 193 (2016).
[11]S. Finizio, M. Foerster, M. Buzzi, B. Krüger, M. Jourdan, C. A. F. Vaz, J. Hockel, T. Miyawaki, A. Tkach, S. Valencia, F. Kronast, G. P. Carman, F. Nolting, and M. Kläui, Phys. Rev. Appl. **1**, 021001 (2014).
[12]P. P. Nguyen and Y. Huai, U.S. Patent 6,985,385 (January 10, 2006).
[13]Y. Telepinsky, V. Mor, M. Schultz, Y. Hung, A. D. Kent, and L. Klein, Appl. Phys. Lett. **108**, 182401 (2016).
[14]M. Dumm, M. Zölfl, R. Moosbühler, M. Brockmann, T. Schmidt, and G. Bayreuther, J. Appl. Phys. **87**, 5457 (2000).
[15]M. Brockmann, S. Miethaner, R. Onderka, M. Köhler, F. Himmelhuber, H. Regensburger, F. Bensch, T. Schweinböck, and G. Bayreuther, J. Appl. Phys. **81**, 5047 (1997).
[16]J. Li, Y. Meng, J. S. Park, C. A. Jenkins, E. Arenholz, A. Scholl, A. Tan, H. Son, H. W. Zhao, C. Hwang, Y. Z. Wu, and Z. Q. Qiu, Phys. Rev. B **84**, 094447 (2011).
[17]C. Won, Y. Z. Wu, W. H. W. Zhao, A. Scholl, A. Doran, W. Kim, T. L. Owens, X. F. Jin, and Z. Q. Qiu, Phys. Rev. B **71**, 024406 (2005).
[18]G. Chen, J. Li, F. Z. Liu, Y. He, J. Zhu, J. Wu, Z. Q. Qiu, and Y. Z. Wu, J. Appl. Phys. **108**, 073905 (2010).
[19]J. W. Shih, Phys. Rev. **46**, 139 (1934).
[20]N. Miyata, K. Tomotsune, H. Nakada, M. Hagiwara, H. Kadomatsu, and H. Fujiwara, J. Phys. Soc. Jpn. **55**, 946 (1986).
[21]S. S. P. Parkin, C. Kaiser, A. Panchula, P. M. Rice, B. Hughes, M. Samant, and S. Yang, Nat. Mater. **3**, 862 (2004).
[22]S. Yuasa, T. Nagahama, A. Fukushima, Y. Suzuki, and K. Ando, Nat. Mater. **3**, 868 (2004).
[23]Y. Shiota, T. Nozaki, F. Bonell, S. Murakami, T. Shinjo, and Y. Suzuki, Nat. Mater. **11**, 39 (2012).
[24]S. A. Gregory, L. C. Maple, G. B. G. Stenning, T. Hesjedal, G. van der Laan, and G. J. Bowden, Phys. Rev. Appl. **4**, 054015 (2015).
[25]A. A. Baker, A. I. Figueroa, C. J. Love, S. A. Cavill, T. Hesjedal, and G. van der Laan, Phys. Rev. Lett. **116**, 047201 (2016).
[26]Y. V. Goryunov, N. N. Garif'yanov, G. G. Khaliullin, I. A. Garifullin, L. R. Tagirov, F. Schreiber, T. Mühge, and H. Zabel, Phys. Rev. B **52**, 13450 (1995).
[27]T. Kuschel, J. Hamrle, J. Pištora, K. Saito, S. Bosu, Y. Sakuraba, K. Takanashi, and J. Wollschläger, J. Phys. D Appl. Phys. **45**, 495002 (2012).
[28]G. B. G. Stenning, L. R. Shelford, S. A. Cavill, F. Hoffmann, M. Haertinger, T. Hesjedal, G. Woltersdorf, G. J. Bowden, S. A. Gregory, C. H. Back, P. A. J. de Groot, and G. van der Laan, New J. Phys. **17**, 013019 (2015).
[29]J. Li, E. Jin, H. Son, A. Tan, W. N. Cao, C. Hwang, and Z. Q. Qiu, Rev. Sci. Instrum. **83**, 033906 (2012).
[30]R. S. Sundar and S. C. Deevi, Int. Mater. Rev. **50**, 157 (2005).